Chapter-6

Energy, Exergy and Environmental (3E) Assessments of a Tea-leaf Withering Trough Coupled with a Solar Air Heater with Two Different Absorber Plates

Among the many renewable energy sources, solar energy is one of the commonly used non-conventional sources for drying. There have been quite a lot of literature found on such type of solar drying of various agro-based products. It becomes essential to assess both the energy as well as exergetic performances in the drying processes. In most of the studies made in this field, both energy and exergy analyses of the drying processes are looked upon. The quantity of energy required is known from the energy analysis. However, the causes for irreversibility may only be achieved from the exergy analysis. The discussions on the studies made on some exergy analyses of solar drying practices are done in the literature review chapter. Studies on solar thermal energy utilization for heating water [150], thermo-hydraulic properties [53], improved solar air heaters [154,157,163,200], parabolic collectors and solar water purification [55,64], solar cookers [199] etc., have been reported. The aspect of drying tea using renewable energy has been explored to certain extent, however there is a gap in similar research in the withering operation of tea processing.

Low temperature drying (withering) of tea leaves by the usage of solar thermal energy under North-east Indian climatic perspective is not available from the literature as such. The chapter focuses on withering of tea leaves in a laboratory set-up of tea-leaf withering trough coupled with an SAH. The energy and exergy analyses of the trough using two types of absorber plates have been done- a corrugated plate and a plate having Al-can protrusions in it. Further, an environmental analysis has been conducted for the arrangement.

6.1 Materials and methods

Green tea leaves withering was performed in a solar energy powered laboratory scale withering trough set-up. The experiments were carried out in the Mechanical Engineering Department of Tezpur University (26°65'28" N, 92°79'26" E), India. The experiments on the SAH were conducted according to the ANSI/ASHRAE Standard 93-2003 for evaluating the thermal enactment of solar collectors [14]. Fresh green tea leaves

were kept sealed under refrigeration for preventing moisture loss after collection from a local tea garden. The tea leaves were equally weighed and placed on three trays. These sample trays were mounted upon a perforated tray in the withering chamber. A digital weighing balance was used to weigh the sample trays after every half hour. This process was continued till the moisture content had reached the desired value. The readings were taken as the average of three repetitions of the experiments. The withering temperature was maintained around 308 K with a relative humidity range of (75-85) % in the trough.

Corrugated SAH absorber increases convective heat transfer to air due to breaking (turbulence) of laminar sub-layer. Al-can solar thermal absorber increases the surface area (like cylindrical fin) and create local turbulence to the airflow. These two factors enhance heat transfer into the flowing air over the Al- can absorber. As a result, Al-can is expected to give better heat transfer performance. Both corrugated absorber and Al-cans are readily available and inexpensive. By using these materials, the overall SAH development cost is reduced with high performance. Utilizing Al-cans for the absorber plates reduces waste and promotes recycling.

The withering trough was coupled with an SAH, first with a corrugated absorber plate with exposed area of 1.41 m^2 and then with an absorber plate containing waste Al-cans. The Al-can absorber plate was added with 53 cylindrical elements made from waste Al-cans, having *e* and *d* dimensions of 40 mm and 53 mm respectively [14, 221-224]. The tilt angle was kept around 27° for the experiments. Three mass flow rates of 0.03, 0.04 and 0.05 kg/s were considered for conducting the experiments in both the cases. Fig. 6.1 shows the schematic diagram of the tea withering trough having corrugated plate SAH (Type-1). Fig. 6.2(a) and 6.2(b) show the schematics of the Al-can SAH and the dimensions of the cylindrical elements respectively. Fig. 6.3 shows the schematic diagram of the tea withering trough coupled with Al-can plate SAH (Type-2). The relative humidity and temperatures were recorded using thermo-hygrometers. An anemometer was used to measure air velocities and a pyranometer recorded the solar radiation. The technical details of the equipment used are given in Table-5.2 in Chapter-5. Fig. 6.4(a) is the top view of the Al-can SAH and Fig. 6.4(b) is the SAH with Al-can absorber plate. The geometrical parameters considered for the Type-2 SAH are given in Table-6.1.

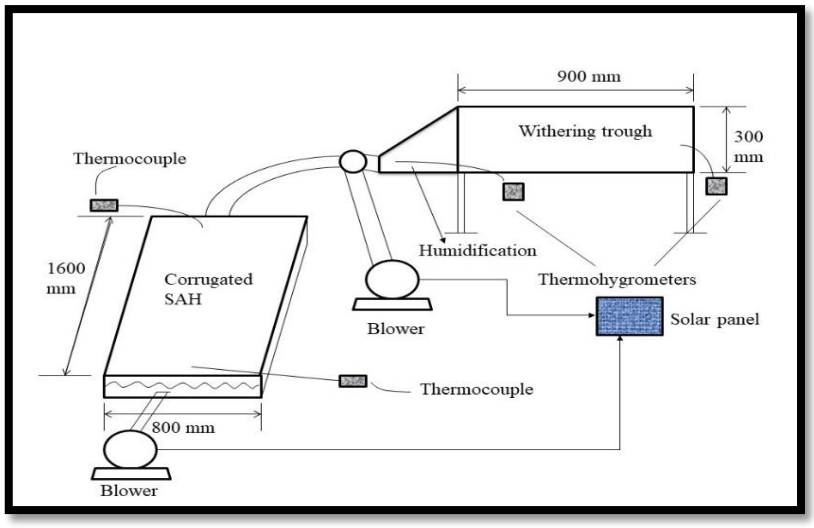

Fig. 6.1. Schematic diagram of the tea withering trough with corrugated plate SAH

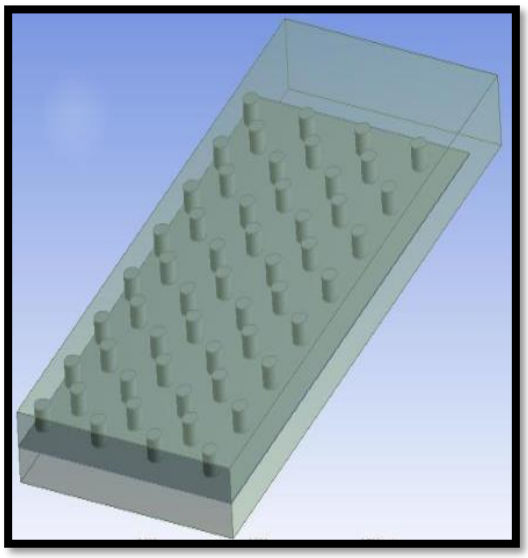

Fig. 6.2(a). SAH with cylindrical elements from Al cans

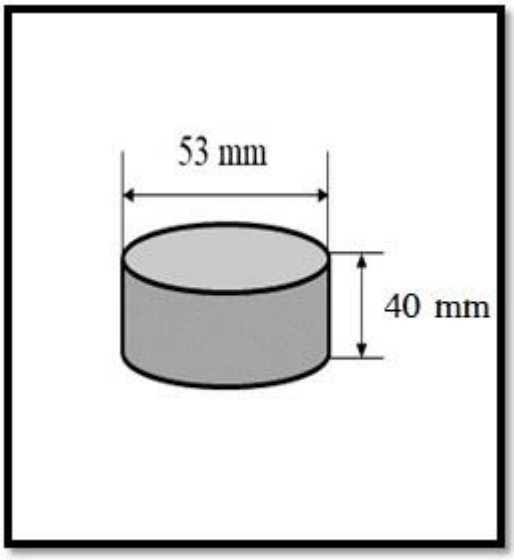

Fig. 6.2(b). Cylindrical element

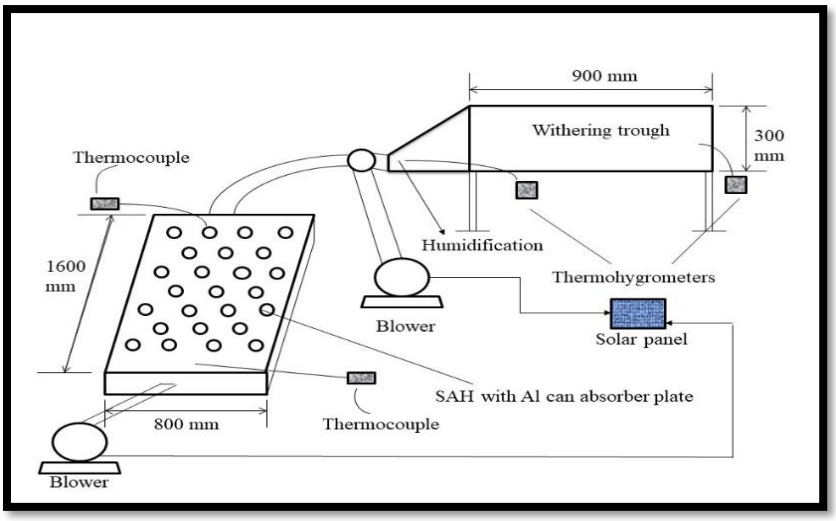

Fig. 6.3. Schematic diagram of the tea withering trough with Al-can plate SAH

Table-6.1. Geometrical parameters of the Al-can absorber plate

Parameters	**Value**
Relative short way length (S/e)	4
Relative long way length (L/e)	4.4
Relative print diameter (d/e)	1.32
Duct Aspect ratio (W/H)	17.5

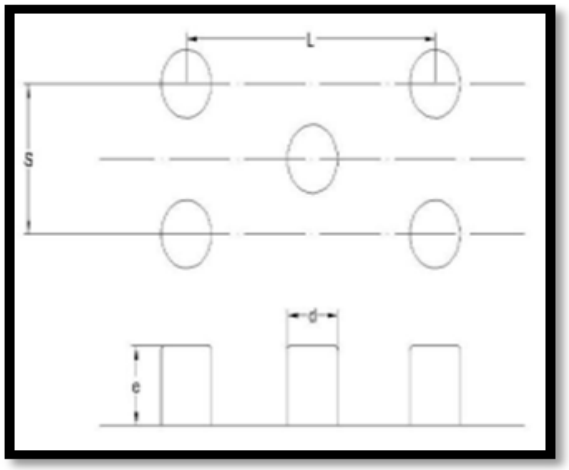

Fig. 6.4(a). Arrangement of cylindrical geometry fabricated on the absorber plate

Fig. 6.4(b). SAH with Al-can absorber plate

6.1.1 Losses in a solar air heater

The solar air heater was subjected to various losses during the experiments. The overall heat loss coefficient (U_{over}) is given by [182] -

$$U_{over} = U_T + U_B + U_E \tag{6.1}$$

where, U_T, U_B and U_E are the top, bottom, and edge losses respectively.

The top loss coefficient is given by Eq.(6.2) [182]-

$$U_T = \left[\left(\frac{1}{h_1}\right) + \left(\frac{1}{h_2}\right)\right]^{-1} \tag{6.2}$$

where, h_1 and h_2 are the total heat transfer coefficients from collector plate to cover and from cover to ambient respectively. The values of h_1 and h_2 are determined by Eq.(6.3) and Eq.(6.4) respectively [182]-

$$h_1 = \frac{Nu.K}{L} + \sigma.\left(\frac{1}{\varepsilon_p} + \frac{1}{\varepsilon_g} - 1\right)^{-1}.\left[\frac{\left(T_p + 273\right)^4 - \left(T_g + 273\right)^4}{T_p - T_g}\right] \tag{6.3}$$

where, Nu is the Nusselt number, K is the thermal conductivity of air (W/m K), L is the spacing between plate and cover (m), T_p and T_g are the mean temperatures of plate and glass cover (°C), ε_p and ε_g are the emissivity of plate and glass respectively (= 0.9 and 0.88 respectively), σ is the Stefan-Boltzmann constant (= 5.67×10^{-8} W/m^2 K^4).

$$h_2 = h_w + \sigma.\varepsilon_g.\left[\frac{\left(T_g + 273\right)^4 - \left(T_{sky} + 273\right)^4}{T_g - T_e}\right] \tag{6.4}$$

where, T_e is the ambient temperature and T_{sky} is the sky temperature (= T_e - 6) in °C [182].

$$h_w = 5.7 + 3.8v_w \tag{6.5}$$

where, h_w is the wind heat transfer coefficient (W/m^{2}K) and v_w is the wind velocity (= 1 m/s) [182].

The bottom loss coefficient is calculated by Eq.(6.6) as [182]-

$$U_B = \left[\left(\frac{L_{in}}{K_{in}}\right) + \left(\frac{1}{h_b}\right)\right]^{-1} \tag{6.6}$$

where, L_{in} and K_{in} are the length (= 0.025 m) and conductivity of insulation (= 0.03 W/mK for dry wood) respectively and h_b is the heat loss coefficient from the bottom. The second

term of this equation may be neglected as compared to the first, thus resulting in Eq. (6.7) [182]-

$$U_B = \left[\left(\frac{L_{in}}{K_{in}} \right) \right]^{-1} \tag{6.7}$$

The edge loss coefficient is calculated by Eq. (6.8) [182]-

$$U_E = U_B \left(\frac{A_E}{A_S} \right) \tag{6.8}$$

where, A_E and A_S are the edge area and collector area respectively.

6.1.2 Energy analysis of the SAH

From the conservation of mass for drying medium [4],

$$\sum \dot{m}_{ai} = \sum \dot{m}_{ao} = \sum \dot{m}_{air} \tag{6.9}$$

Amount of useful heat gained by the SAH is given by [4]-

$$Q_u = \dot{m}_{air} C_p (T_o - T_i) \tag{6.10}$$

The average thermal efficiency of the SAH is given by [4]-

$$\eta_{SAH_{avg}} = \frac{\dot{m}_{air} C_p (T_o - T_i)}{\alpha \tau I_S A_S} \tag{6.11}$$

6.1.3 Thermo-hydraulic performance parameter

Thermo-hydraulic performance parameter ($THPP$) is defined to evaluate the hydrothermal performance of an SAH with different geometry compared to that of a flat-plate SAH. The $THPP$ measures the relative increase in Nusselt number in the modified absorbers to the pressure drop (pumping power expenditure) due to the presence of hindrances over a flat plate absorber. If this ratio exceeds 1, it indicates a potential advantage of using a modified absorber over a conventional flat plate absorber. The *THPP* is expressed by Eq. (6.12) as [214]-

$$THPP = \frac{Nu_{MSAH} / Nu_{FSAH}}{\left(f_{MSAH} / f_{FSAH} \right)^{1/3}} \tag{6.12}$$

where, Nu_{MSAH} and Nu_{FSAH} are the Nusselt numbers for modified and flat plate absorbers respectively. Nu_{MSAH} is calculated using Eq. (6.13) as [215]-

$$Nu_{MSAH} = \frac{hD_h}{K} \tag{6.13}$$

where, D_h is the hydraulic diameter of the duct (m), K is the thermal conductivity (W/mK) and h is coefficient of heat transfer (W/m^{2}K) given by Eq. (6.14) [216]-

$$h = \frac{\dot{H}_{SAH}}{A_{ab}\left(T_{MP} - T_{avg}\right)} \tag{6.14}$$

where, $\dot{H}_{SAH}$ is the useful heat gained, T_{MP} and T_{avg} are the mean plate temperature and the average temperature between inlet and outlet respectively.

f_{MSAH} is the friction factor of the modified absorber plate and is given by Eq. 6.15 [217]-

$$f_{MSAH} = \frac{\left(\Delta P / L\right) D}{2\rho u^2} \tag{6.15}$$

Nu_{FSAH} is expressed as $Nu_{FSAH} = 0.023\,\mathrm{Re}^{0.8}\,\mathrm{Pr}^{0.4}$ [218] and the friction factor of flat absorber is expressed by the modified Blasius equation as $f_{FSAH} = 0.0791\,\mathrm{Re}^{-0.25}$ [219].

6.1.4 Exergy analysis of the SAH

Rate of irreversibility (I) is given by [4]-

$$\dot{I} = \dot{E}x_h - \dot{E}x_w + \dot{E}x_i - \dot{E}x_o \tag{6.16}$$

where,

$$\dot{E}x_h = \sum \left[1 - \frac{T_e}{T_S} \right] Q_h \tag{6.17}$$

$$\dot{E}x_i = \sum \dot{m}_i \left[(h_i - h_e) - T_e \left(s_i - s_e \right) \right] \tag{6.18}$$

$$\dot{E}x_o = \sum \dot{m}_o \left[(h_o - h_e) - T_e \left(s_o - s_e \right) \right] \tag{6.19}$$

It is assumed that,

$$\dot{E}x_w = 0 \tag{6.20}$$

$$\sum \dot{m}_i = \sum \dot{m}_o = \sum \dot{m}_{air} \tag{6.21}$$

Substituting the values of Eq.(6.17) to Eq.(6.21) in Eq.(6.16), we get,

$$\dot{I} = \left[1 - \frac{T_e}{T_S} \right] Q_h - \dot{m}_{air} \left[(h_o - h_i) - T_e \left(s_o - s_i \right) \right] \tag{6.22}$$

where, Q_h is the rate of energy received by the solar air heater from solar radiation and is given by [4],

$$Q_h = \alpha \tau A_s I_s \tag{6.23}$$

Enthalpy and entropy changes are respectively obtained by [4]-

$$h_o - h_i = \left(C_{p,o} T_o - C_{p,i} T_i \right) \tag{6.24}$$

$$s_o - s_i = C_p \ln \left(\frac{T_o}{T_i} \right) - R \ln \left(\frac{P_o}{P_i} \right) \tag{6.25}$$

The rate of irreversibility will be finally given by [4]-

$$\dot{I} = \left[1 - \frac{T_e}{T_S} \right] Q_h - \dot{m}_{air} \left(C_{p,o} T_o - C_{p,i} T_i \right) + \dot{m}_{air} T_e C_p \ln \left(\frac{T_o}{T_i} \right) - \dot{m}_{air} T_e R \ln \left(\frac{P_o}{P_i} \right) = \dot{E}x_{des} \tag{6.26}$$

Irreversibility can be directly evaluated by [4]-

$$\dot{E}x_{des} = T_e s_{gen} \tag{6.27}$$

Second law efficiency is [4]-

$$\psi_{SAH} = \frac{\dot{E}x_i}{\dot{E}x_o} = \frac{\dot{m}_{air}\left(\Delta h - T_e \Delta s\right)}{\left(1 - \frac{T_e}{T_S}\right) Q_h} \tag{6.28}$$

6.1.5 Exergy analysis of withering chamber

The general exergy analysis equation is given by [106]-

$$\sum \dot{E}x_i - \sum \dot{E}x_o = \sum \dot{E}x_{des} \tag{6.29}$$

where, $\dot{E}x_{des}$ is the rate of exergy destruction.

The drying air exergies are calculated by [106]-

$$\dot{E}x_{ic} = \dot{m}_{air} C_p \left[\left(T_{ic} - T_e\right) - T_e \ln\left(\frac{T_{ic}}{T_e}\right)\right] \tag{6.30}$$

$$\dot{E}x_{oc} = \dot{m}_{air} C_p \left[\left(T_{oc} - T_e\right) - T_e \ln\left(\frac{T_{oc}}{T_e}\right)\right] \tag{6.31}$$

Exergy losses are evaluated by [106]-

$$\dot{E}x_L = \dot{E}x_{ic} - \dot{E}x_{oc} \tag{6.32}$$

The exergy efficiency of the withering chamber is computed by [106]-

$$\psi_c = \frac{\dot{E}x_{oc}}{\dot{E}x_{ic}} \tag{6.33}$$

6.1.6 Exergy sustainability indicators

Sustainability indicators reflect the effect of the exergy efficiency and the losses on the sustainability of the drying process. Such types are- improvement potential (*IP*), waste exergy ratio (*WER*) and sustainability index (*SI*). These are evaluated using the following relations [191]-

$$IP = \left(1 - \psi_c\right) \dot{E}x_L \tag{6.34}$$

$$WER = \frac{\dot{Ex}_L}{\dot{Ex}_{ic}} \tag{6.35}$$

$$SI = \frac{1}{1-\psi_c} \tag{6.36}$$

6.1.7 Uncertainty analysis

Errors in the experiments can result from the choice of the instrument, the state of the environment, the observations and the readings. The purpose of this analysis is to find mistakes in the estimated amounts derived from the measured values. The uncertainty in the dependent variable is determined by Eq. (6.37)-

$$\Delta Y = \pm\sqrt{\left(\frac{\partial Y}{\partial X_1}\Delta X_1\right)^2 + \left(\frac{\partial Y}{\partial X_2}\Delta X_2\right)^2 + \ldots\ldots\ldots\ldots\left(\frac{\partial Y}{\partial X_n}\Delta X_n\right)^2} \tag{6.37}$$

where, ΔY is the uncertainty in the estimated value and ΔX_1, ΔX_2, ..., ΔX_n are the errors in the independent variables [79].

6.1.8 Environmental impact assessment

Solar energy is considered eco-friendly and one of the cleanest forms of renewable energy. Any drying system associated with solar energy may be assumed energy efficient. The extent to which the system is energy effective can be evaluated by the environmental impact assessment consisting of parameters like embodied energy, energy payback period and greenhouse gas production. The estimation of these parameters is illustrated below-

6.1.8a Energy payback time

The time needed for paying back the energy utilized for the raw materials' production for developing the system is termed as the energy payback time (E_P). It is estimated by [191]-

$$E_P = \frac{E_m}{E_{a,out}} \tag{6.38}$$

where, E_m is the embodied energy (kWh) and $E_{a,out}$ is the annual energy output (kWh/year) of the system and it is given by [191]-

$$E_{a,out} = E_{d,out} \times N_s \tag{6.39}$$

where, N_s is the number of sunshine days in a year (approx. 250) and $E_{d,out}$ is the daily thermal output (kWh) which is calculated by [191]-

$$E_{d,out} = \frac{M_w h_{fg}}{3.6 \times 10^6} \tag{6.40}$$

where, M_w is the moisture evaporated (kg) and h_{fg} is the latent heat of evaporation (J/kg).

6.1.8b Carbon dioxide (CO_2) emission

The emission of CO_2 per annum is estimated using the following relation [191]-

$$CO_2 emmision / year = \frac{E_m \times 0.98}{L_y} \tag{6.41}$$

where, the approximate emission of CO_2 in generation of electricity by coal on an average is 0.98 kg/kWh and L_y is the lifetime of the drying system (years).

If transmission losses (L_T) and domestic appliance losses (L_D) are considered as 40% and 20% respectively, then Eq. (6.41) becomes [191]-

$$CO_2 emmision / year = \frac{E_m}{L_y} \times \frac{1}{1 - L_D} \times \frac{1}{1 - L_T} \times 0.98 \tag{6.42}$$

Substituting the assumed values of losses in Eq. (6.42), the relation finally becomes [191]-

$$CO_2 emmision / year = \frac{E_m \times 2.042}{L_y} kg \tag{6.43}$$

6.1.8c CO_2 mitigation

The CO_2 mitigation per annum considering the transmission and domestic losses can be estimated by [191]-

$$CO_2 mitigation / year = \left(E_{a,out} \times L_y - E_m \right) \times 2.042 kg \tag{6.44}$$

6.1.8d Carbon credit earned

The mitigation of 1 t of CO_2 emission is termed as one carbon credit. The carbon credit earned (*ECC*) by the drying system is given by the product of net CO_2 mitigation in the lifetime and the price of CO_2 mitigation/t as given below [191]-

$$ECC = \left(CO_2 mitigation\right)_{net} \times \left(CO_2 mitigation\right)_{price/t} \quad (6.45)$$

6.2 Results and discussion

6.2.1 Overall loss coefficient of Type-1 SAH

The average overall loss coefficients for the Type-1 SAH were determined for the considered mass flow rates of 0.03, 0.04 and 0.05 kg/s. The variations in the overall loss coefficients are shown in Fig. 6.5.

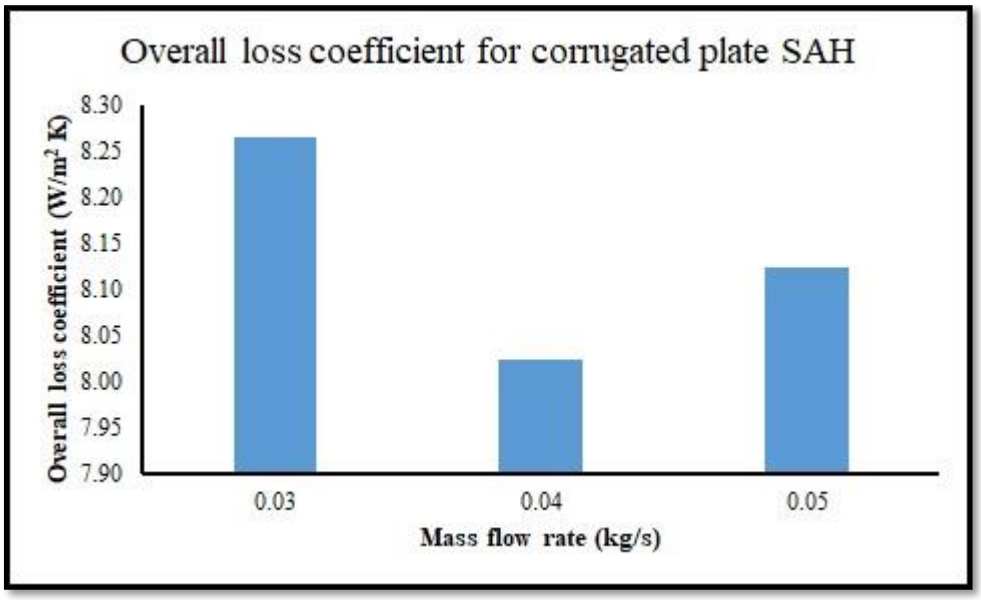

Fig. 6.5. Overall loss coefficient at the three mass flow rates for Type-1 SAH

The average plate temperatures at the mass flow rates were recorded as 118, 110 and 114 ℃ respectively. The bottom and edge loss coefficients were obtained as 1.20 and 0.66 W/m^2 K respectively. The top loss coefficients for the respective mass flow rates were obtained as 6.40, 6.16 and 6.26 W/m^2 K on an average. It is observed that the mean loss decreases initially as the mass flow rate increases to 0.04 kg/s. However, it increases as the mass flow rate rises from 0.04 to 0.05 kg/s. This may be explained due to more temperature gain and heat loss by the absorber plate and glass at 0.05 kg/s resulting in lesser heat gain by the air at a higher velocity. Evidently, the minimum overall loss of 8.02

W/m^2 K was observed at the mass flow rate of 0.04 kg/s that is expected to give better efficacy than the rest conditions.

6.2.2 Energy and exergy analyses of the Type-1 SAH

The withering of freshly plucked tea leaves was done in a laboratory scaled solar thermal energy powered tea-leaf withering trough coupled with a corrugated plate SAH. The mass flow rates of 0.03, 0.04 and 0.05 kg/s were considered for the experiments based on the preferable operating ranges of a solar-powered tea-leaf withering trough as per design. The results obtained for the energy analysis of the Type-1 SAH are presented graphically below-

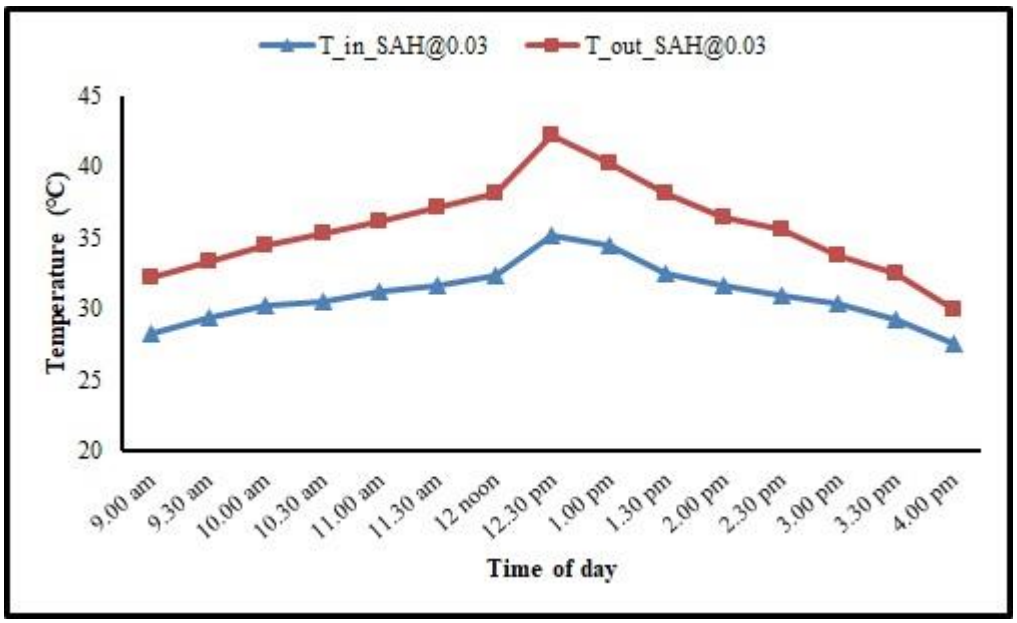

Fig. 6.6(a). Temperature variation in Type-1 SAH at 0.03 kg/s

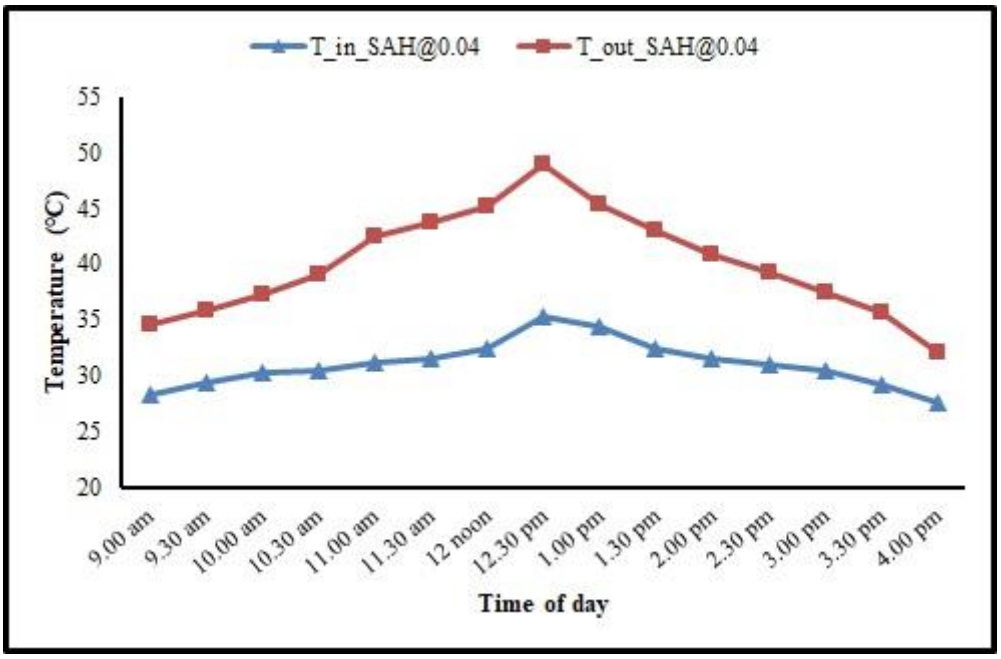

Fig. 6.6(b). Temperature variation in Type-1 SAH at 0.04 kg/s

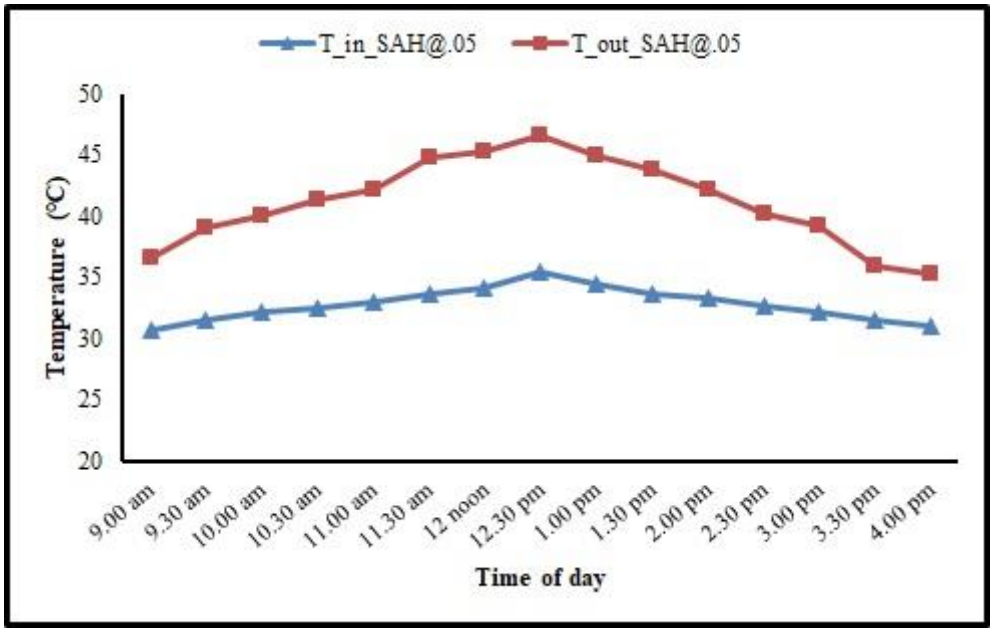

Fig. 6.6(c). Temperature variation in Type-1 SAH at 0.05 kg/s

Figures 6.6(a)-6.6(c) show that the maximum temperatures at the outlet are respectively 42.2 ℃, 49 ℃ and 46.6 ℃ for the mass flow rates of 0.03, 0.04 and 0.05 kg/s. The outlet temperature was the highest at 12.30 PM in all the instances. The corresponding temperature differences between the inlet and outlet were 7 ℃, 13.8 ℃ and 11.2 ℃ for the three cases. The temperature at the outlet decreased as there are heat losses occurring due to less gain of temperature by the air and lower residence time of air at 0.05 kg/s.

Abuska and Raam Dheep and Sreekumar reported such trends in the rise in temperature with mass flow rates [4,143].

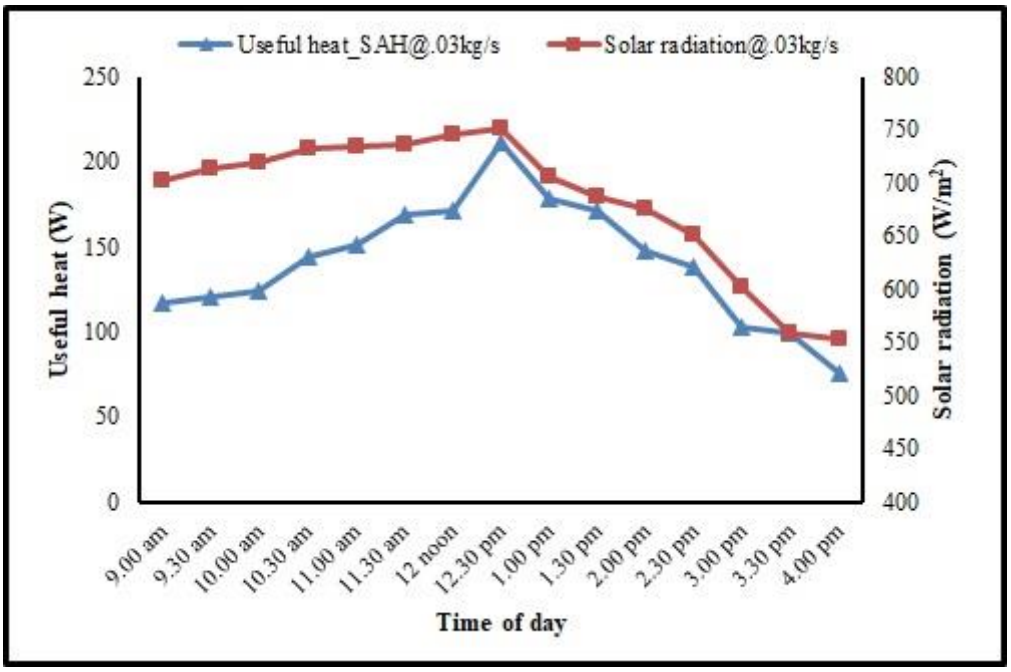

Fig. 6.7(a). Useful heat gain and solar radiation in Type-1 SAH at 0.03 kg/s

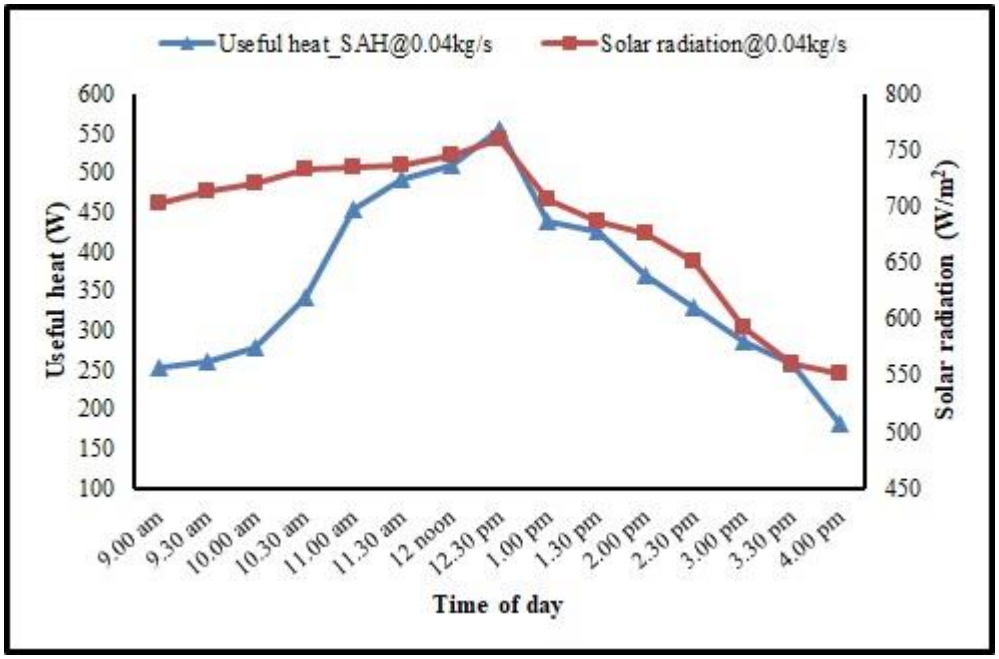

Fig. 6.7(b). Useful heat gain and solar radiation in Type-1 SAH at 0.04 kg/s

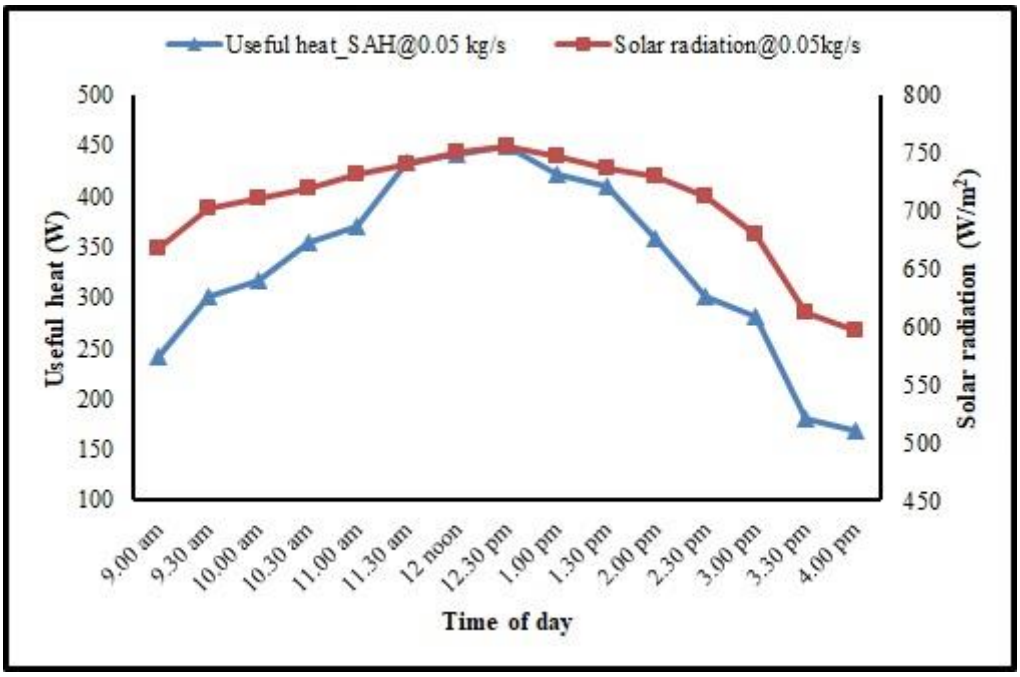

Fig. 6.7(c). Useful heat gain and solar radiation in Type-1 SAH at 0.05 kg/s

Figures 6.7(a)-6.7(c) illustrate the useful heat gained along with the solar radiation at the considered mass flow rates. At 0.03 kg/s, the maximum useful heat gained was 211.1 W at a radiation of 751 W/m^2 as shown in Fig. 6.7(a). Similarly, the maximum useful heat gains were computed as 554.8 W at 759 W/m^2 for 0.04 kg/s and 450.2 W at 755 W/m^2 for 0.05 kg/s as can be seen in Fig. 6.7(b) and Fig. 6.7(c) respectively. Though the solar radiations are in a similar range, the wide variation in the useful heat gained can be explained due to the difference in the mass flow rate and temperature difference between inlet and outlet, thereby contributing to the variations in thermal efficiencies.

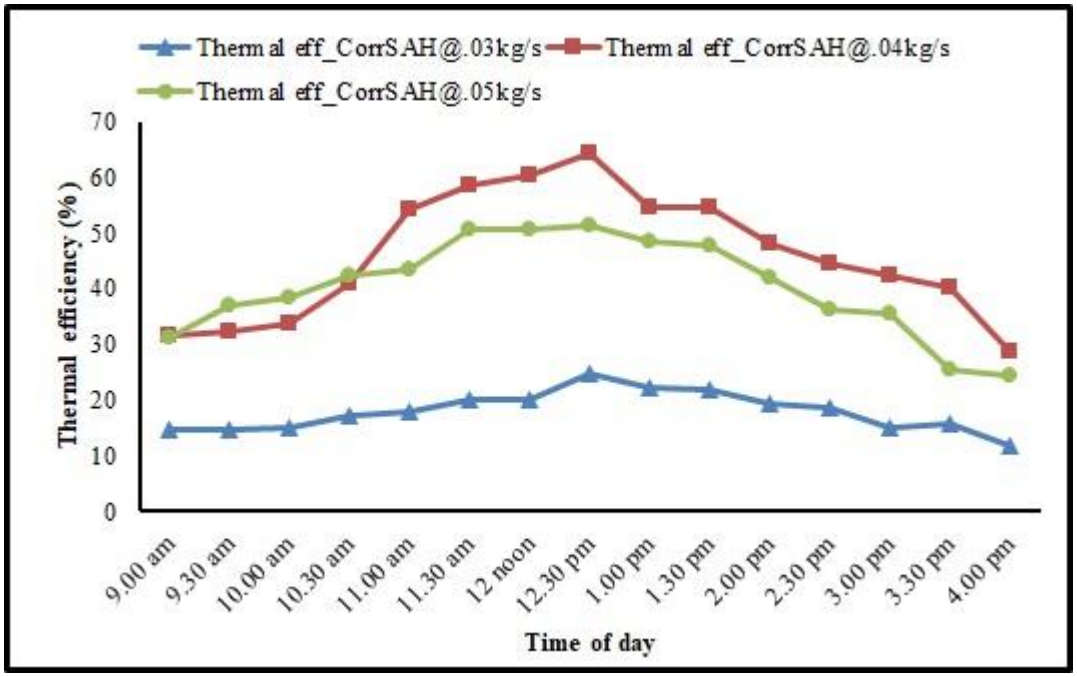

Fig. 6.8(a). Thermal efficiency variation with time of day in Type-1 SAH

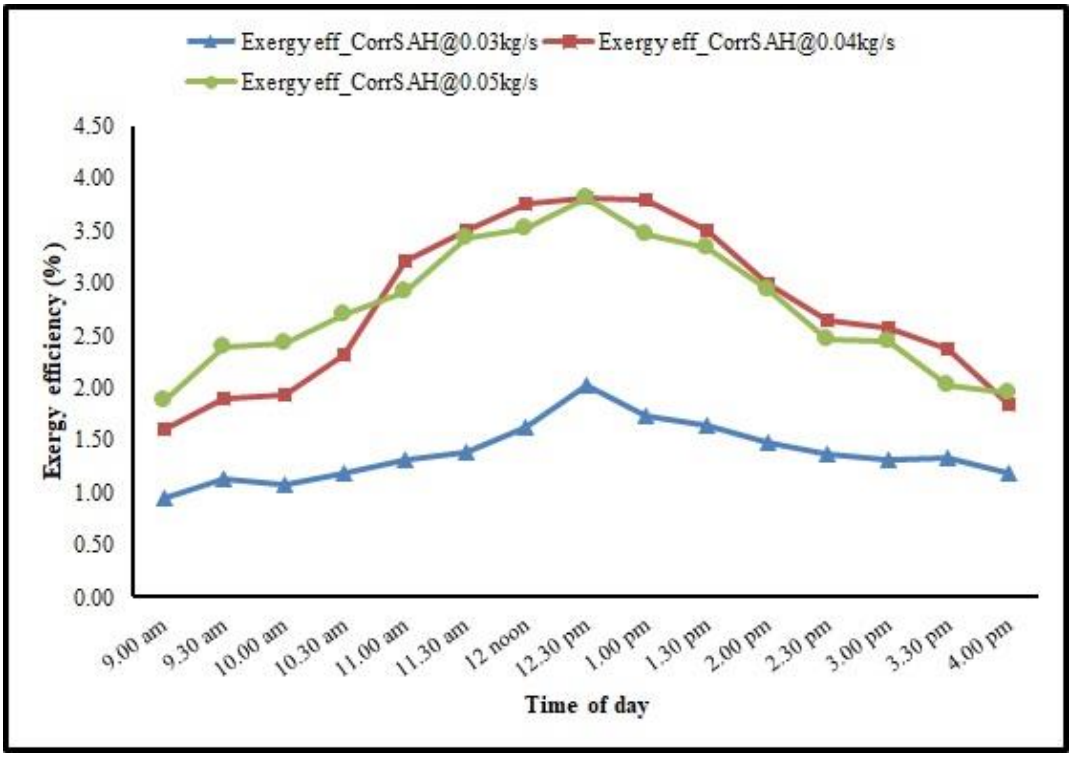

Fig. 6.8(b). Exergy efficiency variation with time of day in Type-1 SAH

The thermal efficiency variation for all the three mass flow rates in the Type-1 SAH is shown in Fig. 6.8(a). At 0.03 and 0.04 kg/s, the maximum thermal efficiencies obtained were 24.68% and 64.2% at solar radiations of 751 W/m^2 and 759 W/m^2

respectively. However, at 0.05 kg/s mass flow rate, the maximum thermal efficiency dropped down to 51.29% at 755 W/m^2. This decrease in efficiency may be explained as the result of lower residence time of air over the absorber. The exergy efficiencies of the SAH at the considered mass flow rates are shown in Fig. 6.8(b). The maximum exergy efficiency obtained at 0.03 kg/s mass flow rate was 2.02%. At 0.04 and 0.05 kg/s, the highest exergy efficiency values were 3.82% and 3.8% respectively. Abuska, Gunjo et al. and Hassan et al. obtained similar trends in the variations of thermal and exergy efficiency of the respective types of SAH taken under study by them [4,70,73].

6.2.3 Exergy analysis of the Type-1 tea withering trough

The exergy analysis of the Type-1 solar-powered tea-leaf withering trough was conducted for the three mass flow rates of 0.03, 0.04 and 0.05 kg/s. The results obtained from the analyses are illustrated below graphically-

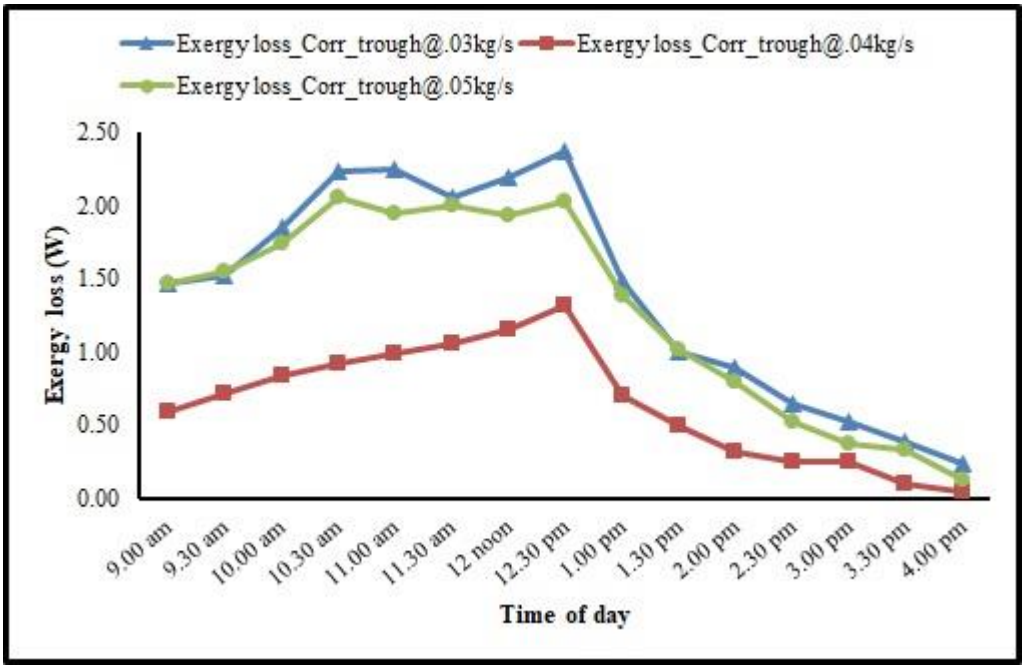

Fig. 6.9(a). Exergy loss during the day in Type-1 withering trough

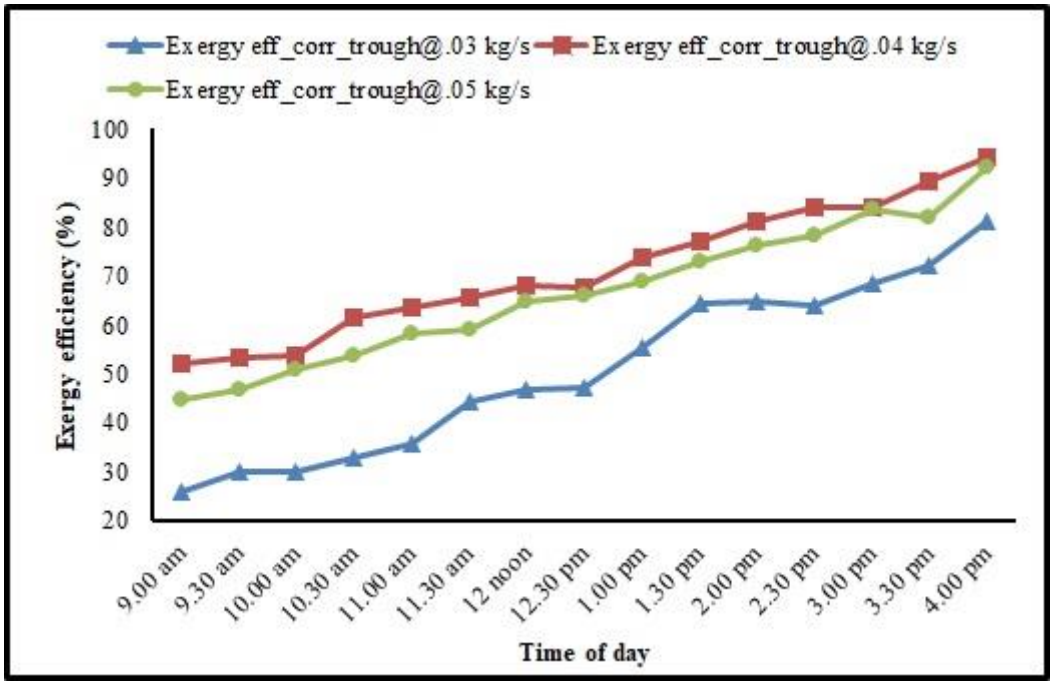

Fig. 6.9(b). Exergy efficiency variation of the Type-1 withering trough during the day

Fig. 6.9(a) shows the variation of exergy loss with the time of the day in the Type-1 withering trough. The mean exergy loss values for the mass flow rates of 0.03, 0.04 and 0.05 kg/s were obtained as 1.41 W, 0.65 W and 1.28 W respectively. The low temperature difference between the inlet and outlet of the withering chamber could be explained as the reason for the lesser values of exergy loss. It is observed from Fig. 6.9(b) that the exergy efficiency of the withering chamber went from 25.98% to 81.09% during the day at 0.03 kg/s. Similarly, the exergy efficiency varied within (52.11-94.23) % at 0.04 kg/s. However, the range of exergy efficiency of the trough was seen comparatively reduced to (44.65-92.20) % at 0.05 kg/s mass flow rate. It is evident as the exergy loss was minimum in the flow rate of 0.04 kg/s. The exergy efficiency increases till the end of the day because of less exergy destruction due to low radiation and temperature. The trends of exergy loss and efficiencies were found tallying with those of [8,142,191].

Table-6.2 gives the exergy sustainability indicators for the Type-1 tea-leaf withering trough. The improvement potential decreases from 0.78 J to 0.22 J as the mass flow rises from 0.03 to 0.04 kg/s. But it increases to 0.51 J at 0.05 kg/s. The waste exergy ratio follows the same trend with the values of 0.49, 0.29 and 0.33. Since the exergy loss is the least at 0.04 kg/s, the potential to improve becomes the lowest at this mass flow rate amongst the other two. Similar is the reason for waste exergy ratio. The sustainability index increases from 2.37 to 4.90 as the mass flow rate rises to 0.04 kg/s but reduces to

3.92 at 0.05 kg/s. It is evident that the mass flow rate of 0.04 kg/s is the most viable for the Type-1 tea-leaf withering trough. The variation in the exergy sustainability indicators are comparable with those of [17,191].

Table-6.2. Exergy sustainability indicators for Type-1 withering trough

Mass flow rate (kg/s)	**IP (J)**	**WER**	**SI**
0.03	0.78	0.49	2.37
0.04	0.22	0.29	4.90
0.05	0.51	0.33	3.92

6.2.4 Overall loss coefficient of the Type-2 SAH

For the tea withering trough set-up with an SAH having Al-can protrusions in the absorber plate, the experiments were conducted for three mass flow rates of 0.03, 0.04 and 0.05 kg/s. The average overall loss coefficients for the Type-2 SAH were determined for the considered mass flow rates. The variations in the overall loss coefficients are shown in Fig. 6.10.

Fig. 6.10. Overall loss coefficient at the three mass flow rates for Type-2 SAH

As seen in Fig. 6.10, the mean plate temperatures at the mass flow rates of 0.03, 0.04 and 0.05 kg/s were recorded as 115, 108 and 112 ℃ respectively. The bottom and edge loss coefficients were obtained as 1.20 and 0.44 $W/m^2 K$ respectively. The top loss

coefficients for the respective mass flow rates were obtained as 6.19, 6.04 and 6.11 W/m^2 K on an average. As in the previous case, it was again observed that the overall loss decreased as the mass flow rate increased to 0.04 kg/s but increased as the mass flow rate rose from 0.04 to 0.05 kg/s. At 0.05 kg/s mass flow rate, less heat transfer took place to the air from the absorber plate due to low residence time, resulting in more heat loss from the absorber. Consequently, the minimum overall loss of 7.68 W/m^2 K was observed at the mass flow rate of 0.04 kg/s, thus showing better effectiveness than the other two rates.

6.2.5 Energy and exergy analyses of the Type-2 SAH

Fresh tea leaves were dried at low temperature, i.e., withered in a laboratory scaled tea-withering trough coupled with a SAH with absorber plate with cylindrical elements of waste Al-cans. Three mass flow rates of 0.03, 0.04 and 0.05 kg/s were considered again in this case. The outcomes of the energy and exergy analyses of the SAH are presented below-

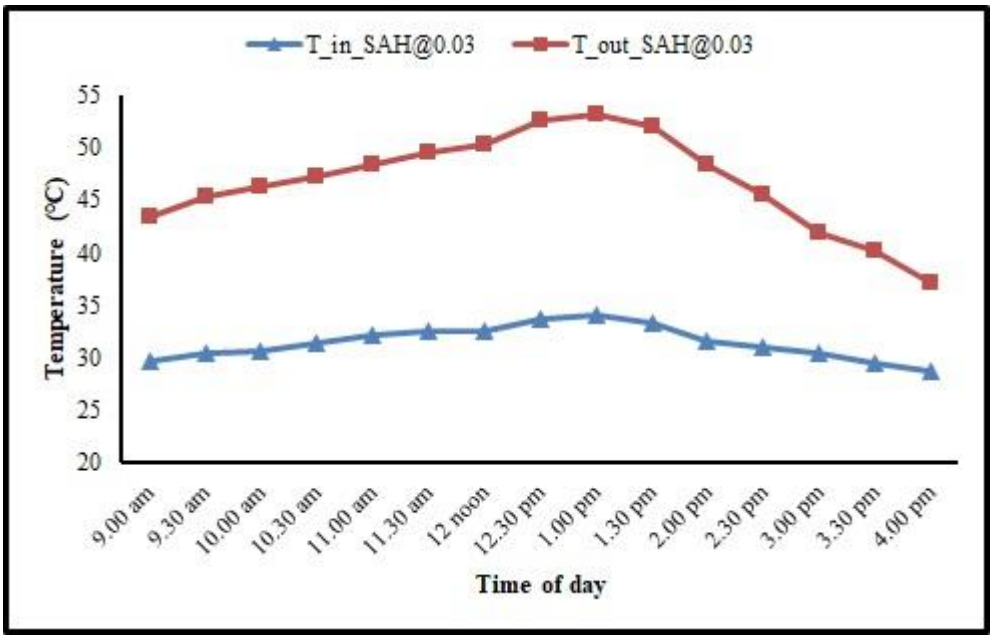

Fig. 6.11(a). Temperature variation in Type-2 SAH at 0.03 kg/s

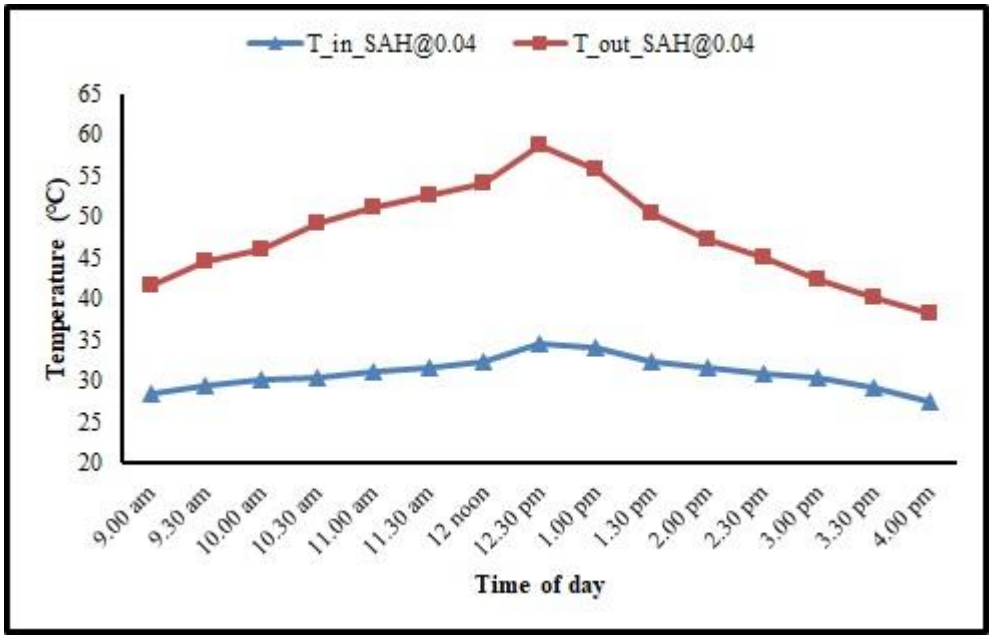

Fig. 6.11(b). Temperature variation in Type-2 SAH at 0.04 kg/s

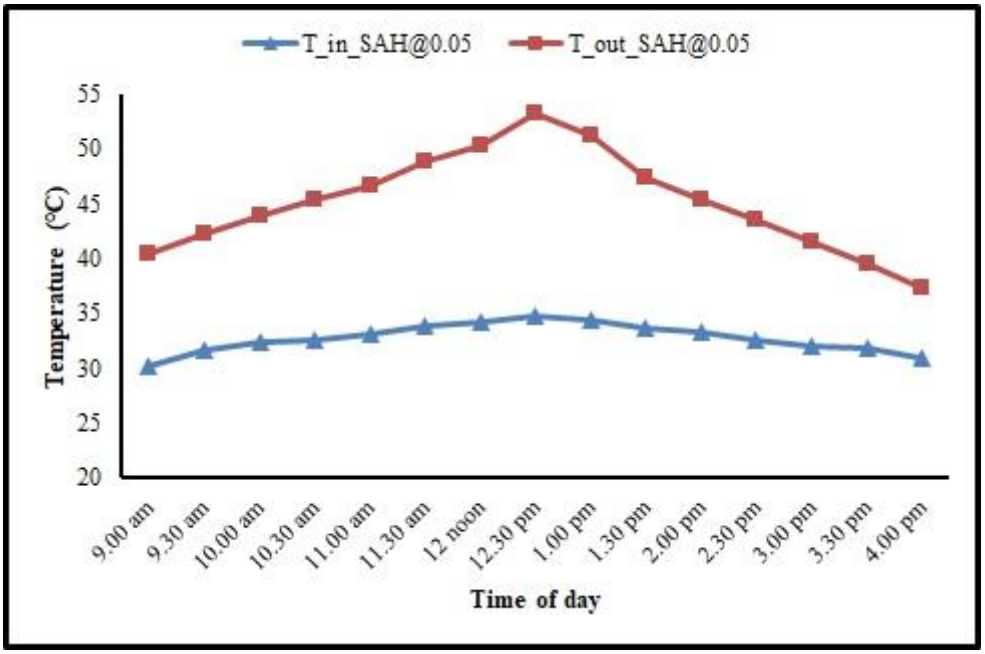

Fig. 6.11(c). Temperature variation in Type-2 SAH at 0.05 kg/s

The maximum temperatures at the outlet of the Type-2 SAH were respectively obtained as 52.1 ℃, 58.7 ℃ and 53.2 ℃ for the mass flow rates of 0.03, 0.04 and 0.05 kg/s as seen in Fig. 6.11(a)-6.11(c). As expected, the temperature difference increased as the mass flow rate increased to 0.04 kg/s. However, there was a slight decrease in the temperature difference at the mass flow rate of 0.05 kg/s. This decline may be due to the less temperature gain of the air due to higher flow rate leading to heat losses. Abuska and

Raam Dheep and Sreekumar reported such trends in the rise in temperature with mass flow rates [4,143].

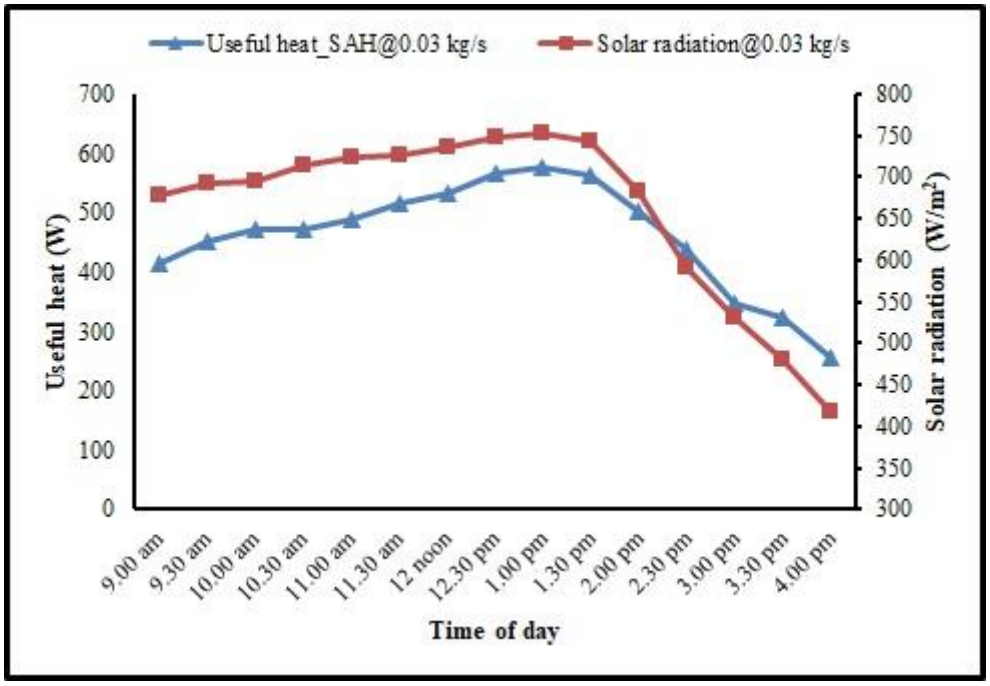

Fig. 6.12(a). Useful heat gain and solar radiation in Type-2 SAH at 0.03 kg/s

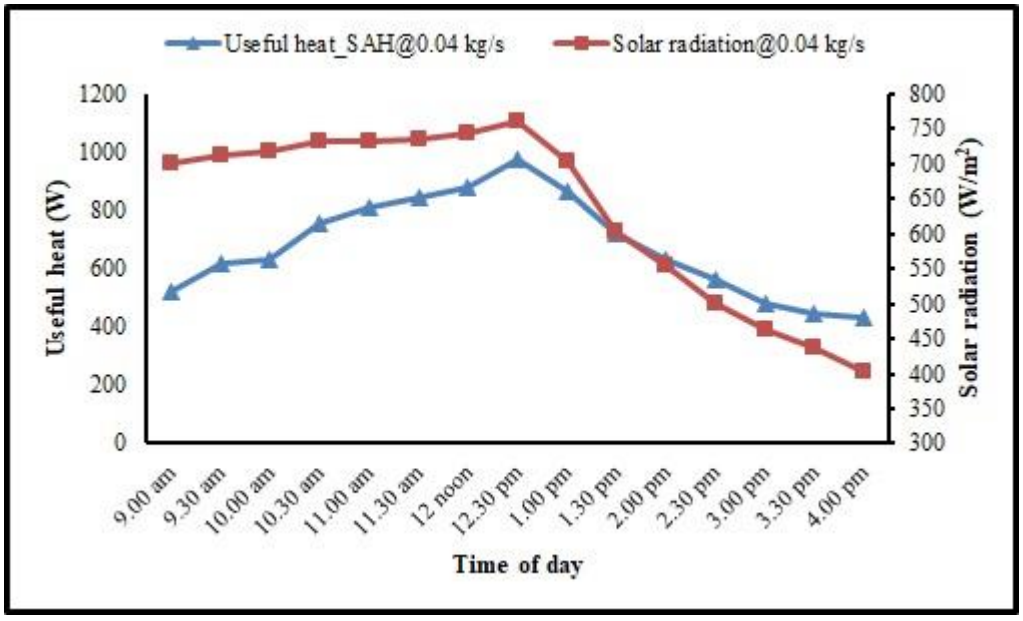

Fig. 6.12(b). Useful heat gain and solar radiation in Type-2 SAH at 0.04 kg/s

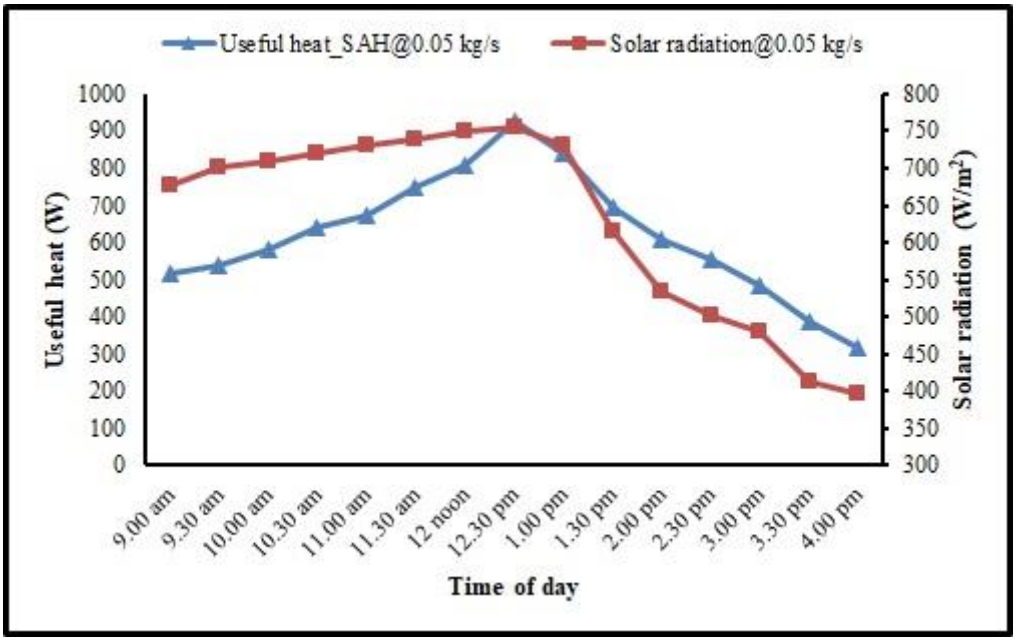

Fig. 6.12(c). Useful heat gain and solar radiation in Type-2 SAH at 0.05 kg/s

Fig. 6.12(a)-6.12(c) illustrate the useful heat gained and the solar radiation at the considered mass flow rates for Type-2 SAH. At 0.03 kg/s, the useful heat gained was obtained the maximum value at a radiation of 752 W/m^2 with a value of 575.8 W as shown in Fig. 6.12(a). The maximum useful heat gains at 0.04 and 0.05 kg/s were obtained as 972.8 W at 760 W/m^2 and 924.6 W at 756 W/m^2 respectively as can be seen in Fig. 6.12(b) and Fig. 6.12(c) respectively. Here again, the difference in the mass flow rate and temperature difference between inlet and outlet is the reason behind the wide variation in the useful heat gained, thus reflecting in the thermal efficiency of the SAH.

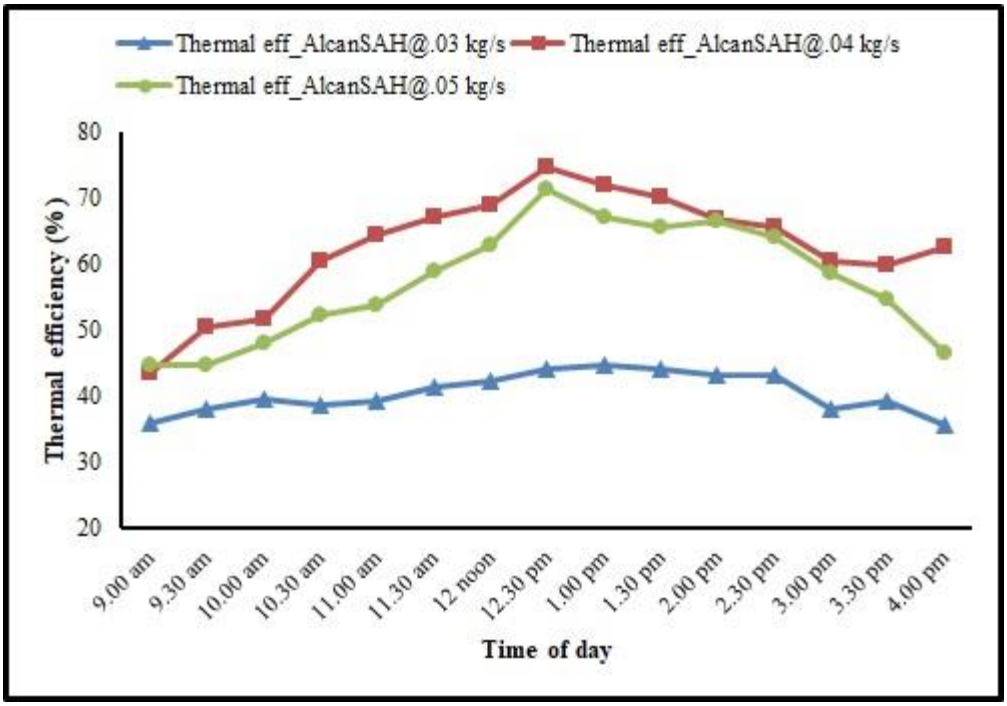

Fig. 6.13(a). Thermal efficiency variation with time of day in Type-2 SAH

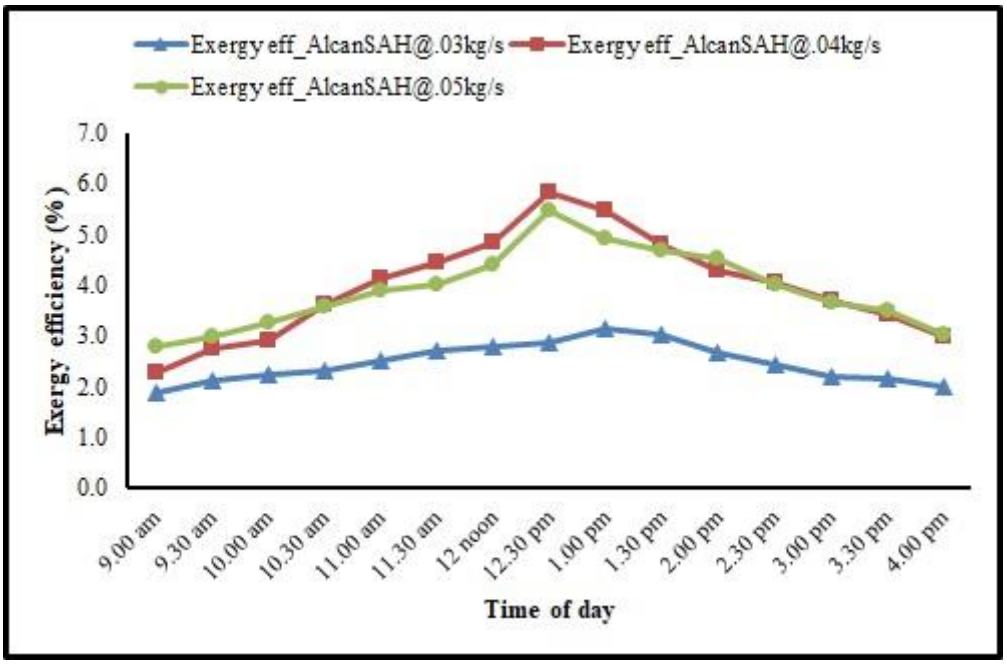

Fig. 6.13(b). Exergy efficiency variation with time of day in Type-2 SAH

Fig. 6.13(a) shows the variation of thermal efficiency for all the three mass flow rates in the Type-2 SAH. At 0.03 kg/s, the maximum thermal efficiency was obtained as 44.73% at solar radiation of 752 W/m^2 and it increased to 74.77% at 760 W/m^2 when the mass flow rate was 0.04 kg/s. However, the maximum thermal efficiency dropped down for 0.05 kg/s mass flow rate to 71.44% at a solar radiation 756 W/m^2. This decrease in

efficiency is evident as the temperature difference between the inlet and outlet of the SAH lessened in this case compared to 0.04 kg/s due to more heat loss. Fig. 6.13(b) shows the exergy efficiencies of the Type-2 SAH at the considered mass flow rates. It is observed that the variation of exergy efficiency at 0.03 kg/s was between (1.87-3.16) %. At 0.04 and 0.05 kg/s, the exergy efficiency varied within the range of (2.28-5.84) % and (2.81-5.49) % respectively. Abuska, Gunjo et al. and Hassan et al. obtained similar trends in the variations of thermal and exergy efficiency of SAHs under study [4,70,73].

6.2.6 Exergetic assessment of the tea withering trough with Type-2 SAH

The exergetic performance of the solar thermal energy powered tea withering trough with Type-2 SAH was carried out for the mass flow rates of 0.03, 0.04 and 0.05 kg/s. The graphical illustrations of the analyses are shown below-

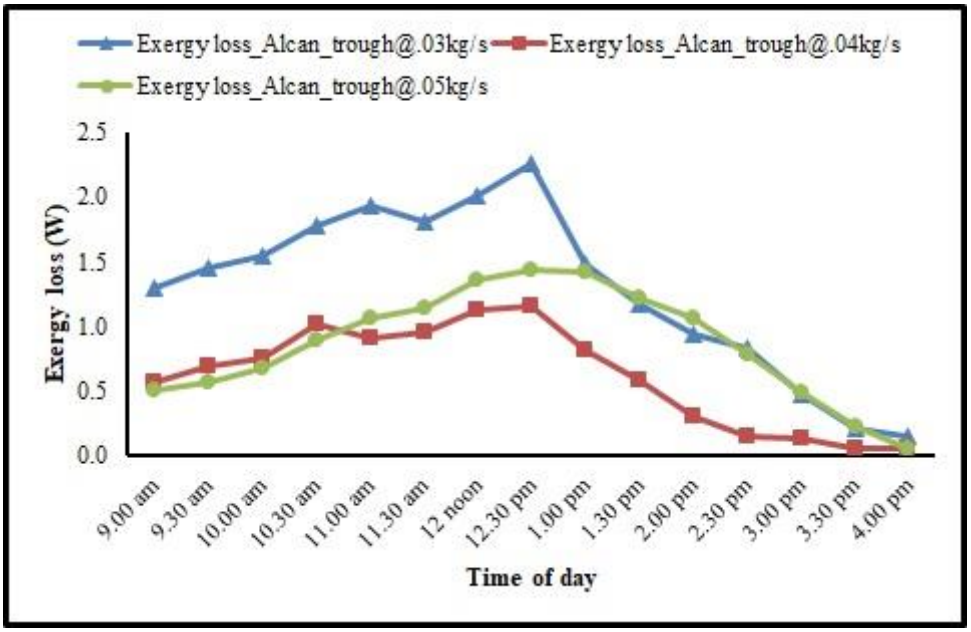

Fig. 6.14(a). Exergy loss during the day in Type-2 withering trough

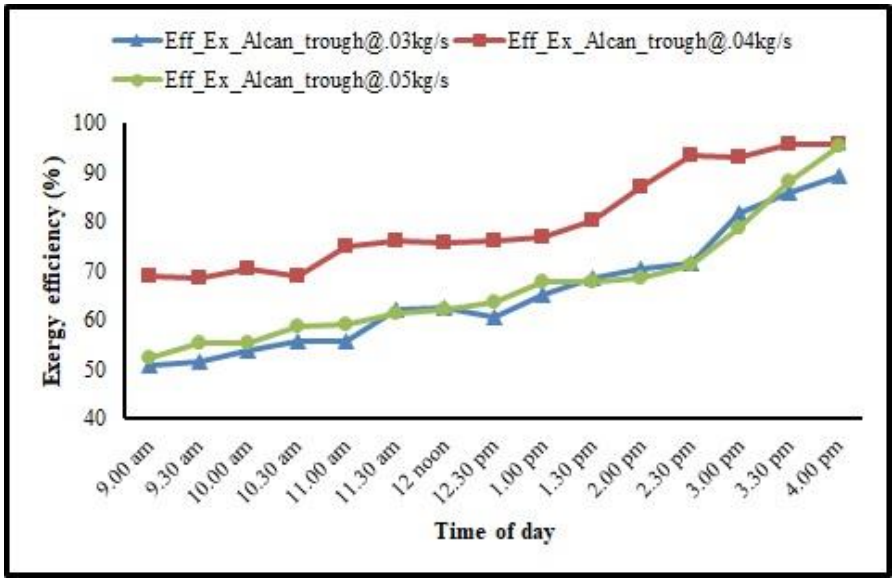

Fig. 6.14(b). Exergy efficiency variation of the Type-2 withering trough during the day

Fig. 6.14(a) shows the variation of exergy loss in the Type-2 withering trough with the time of the day. The mean exergy loss values for the mass flow rates of 0.03, 0.04 and 0.05 kg/s were obtained as 1.29 W, 0.62 W and 0.87 W respectively. The low temperature difference between the inlet and outlet of the withering chamber could be explained to be the reason for the lesser values of exergy loss. At 0.03 kg/s, it is seen from Fig. 6.14(b) that the exergy efficiency of the withering chamber went from 50.98% to 89.26% during the day. The exergy efficiency varied within (69.06-95.63) % at 0.04 kg/s. However, the range of exergy efficiency of the trough was seen to be comparatively reduced to the range of (52.28-95.20) % at 0.05 kg/s mass flow rate. It is clear from the results as the exergy loss was minimum in the flow rate of 0.04 kg/s. The trends of exergy loss and efficiencies were found tallying with those of [8,142,191].

The exergy sustainability indicators for Type-2 withering trough were evaluated for the three mass flow rates considered and given in Table-6.3 below. The improvement potential decreased from 0.51 J to 0.15 J as the mass flow rose from 0.03 to 0.04 kg/s. But it increased to 0.31 J at 0.05 kg/s. The waste exergy ratio followed the same trend with the values of 0.34, 0.20 and 0.33. It happened as these two parameters are related with the exergy loss. This shows that the mass flow rate of 0.04 kg/s has the least potential to be improved, that make it a suitable flow rate to be used. The sustainability index increased from 3.57 to 8.14 as the mass flow rate goes up to 0.04 kg/s but reduced to 4.41 at 0.05 kg/s. These results indicate that the withering chamber has better sustainability for the mass flow rate of 0.04 kg/s compared to the other two. The trends of variation in the exergy

sustainability indicators are comparable with those of [17,191]. Thus, the tea-leaf withering trough coupled with the Al-can plate SAH proves to be more efficient than the corrugated one.

Table-6.3. Exergy sustainability indicators for Type-2 withering trough

Mass flow rate (kg/s)	**IP (J)**	**WER**	**SI**
0.03	0.51	0.34	3.57
0.04	0.15	0.20	8.14
0.05	0.31	0.33	4.41

6.2.7 *THPP* of corrugated and Al-can SAH

The thermo-hydraulic performance parameters ($THPP$) for the corrugated and Al-can SAH is shown in Fig. 6.15. The average $THPP$ is observed to be above 1.0 for both the types of SAH. This indicates that integrating Al-cans or corrugations into a flat plate absorber results in a relatively greater enhancement in the Nusselt number compared to the increase in friction. The results closely align with the observations reported by Madadi et al. [214], which demonstrated that an absorber plate with vertical cylinders had an average THPP of 1.2. In a study of V-rib geometry SAH, the highest $THPP$ was calculated as 1.59 [220].

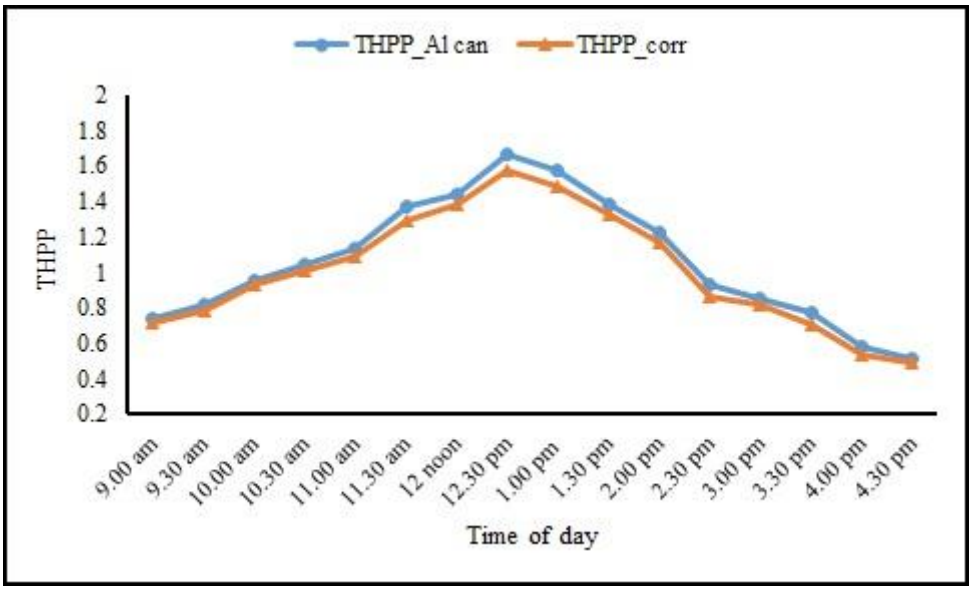

Fig. 6.15. *THPP* of corrugated and Al-can SAH

6.2.8 Uncertainty analysis

The total uncertainty in the thermal efficiency of the SAH and the exergy efficiencies of the SAH and withering chamber were determined by-

$$\Delta\eta_{SAH} = \pm\sqrt{\left(\frac{\partial\eta_{SAH}}{\partial\dot{m}_{air}}\Delta\dot{m}_{air}\right)^2+\left(\frac{\partial\eta_{SAH}}{\partial T_o}\Delta T_o\right)^2+\left(\frac{\partial\eta_{SAH}}{\partial T_i}\Delta T_i\right)^2+\left(\frac{\partial\eta_{SAH}}{\partial I_S}\Delta I_S\right)^2+\left(\frac{\partial\eta_{SAH}}{\partial A_S}\Delta A_S\right)^2} \quad (6.46)$$

$$\Delta\psi_{SAH} = \pm\sqrt{\left(\frac{\partial\psi_{SAH}}{\partial\dot{m}_{air}}\Delta\dot{m}_{air}\right)^2+\left(\frac{\partial\psi_{SAH}}{\partial T_o}\Delta T_o\right)^2+\left(\frac{\partial\psi_{SAH}}{\partial T_i}\Delta T_i\right)^2+\left(\frac{\partial\psi_{SAH}}{\partial P_d}\Delta P_d\right)^2+\left(\frac{\partial\psi_{SAH}}{\partial I_S}\Delta I_S\right)^2+\left(\frac{\partial\psi_{SAH}}{\partial A_S}\Delta A_S\right)^2} \quad (6.47)$$

$$\Delta\psi_c = \pm\sqrt{\left(\frac{\partial\psi_c}{\partial\dot{m}_{air}}\Delta\dot{m}_{air}\right)^2+\left(\frac{\partial\psi_c}{\partial T_{ic}}\Delta T_{ic}\right)^2+\left(\frac{\partial\psi_c}{\partial T_{oc}}\Delta T_{oc}\right)^2} \quad (6.48)$$

where, $\Delta\eta_{SAH}$ is the uncertainty in the thermal efficiency of the solar air heater, $\Delta\Psi_{SAH}$ and $\Delta\Psi_C$ are the uncertainties in the exergy efficiencies of SAH and withering trough respectively. Table-6.4 enlists the mean uncertainties in the different estimated parameters.

Table-6.4. Uncertainty in the estimated parameters

Parameters	**Uncertainty values**
Thermal efficiency of SAH (%)	± 0.14
Exergy efficiency of SAH (%)	± 0.47
Exergy efficiency of withering trough (%)	± 0.65

6.2.9 Environmental assessment

The environmental impact is analyzed for the more efficient Type-2 withering trough which is assumed to be capable of drying 10 kg tea leaves. The total mass of the materials of the set-up is calculated as 81.03 kg. The percentage break-up of the mass is shown in Fig. 6.16(a). The frames constitute the highest percentage of mass in the system with 36.65% followed by casings and the withering chamber with 16.54% and 14.88% respectively. The embodied energy of the materials used in the development of the solar thermal based tea withering trough is detailed in Table-6.5. The total embodied energy is estimated to be 959.99 kWh for the entire system. The break-up in the percentage of embodied energy is detailed in Fig. 6.16(b). Again, the highest share of 27.50% is given by the frames. But the absorber plate shares the second highest in this case with 22.39%

followed by the casings with 12.41%. This happens because aluminum consumes the higher embodied energy than the other materials used [159,191].

Table-6.5. Embodied energy of the materials

Component	**Material**	**Embodied energy (kWh/kg)** [159,191]	**Quantity (kg)**	**Total embodied energy(kWh)**
Glass cover	Glass	7.28	3.60	26.21
Absorber plate	Al	55.28	3.89	214.93
Cans	Al	55.28	0.80	43.95
Withering chamber	GI sheet	9.636	12.06	116.21
Plywood	Wood	2.88	2.34	6.74
Frames	MS	8.89	29.70	264.03
Trays	SS mesh	8.89	11.25	100.01
Fittings (nuts, bolts etc.)	Steel	8.89	1.00	8.89
Cu wire (blower)	Cu	19.61	0.50	9.81
Casings, fan etc. (blower)	Steel	8.89	13.40	119.13
Piping	PVC	19.39	0.50	9.70
Coating	Paint	25.11	1.00	25.11
Insulation in chamber	Cotton	15.28	1	15.28
Total embodied energy=				**959.99**

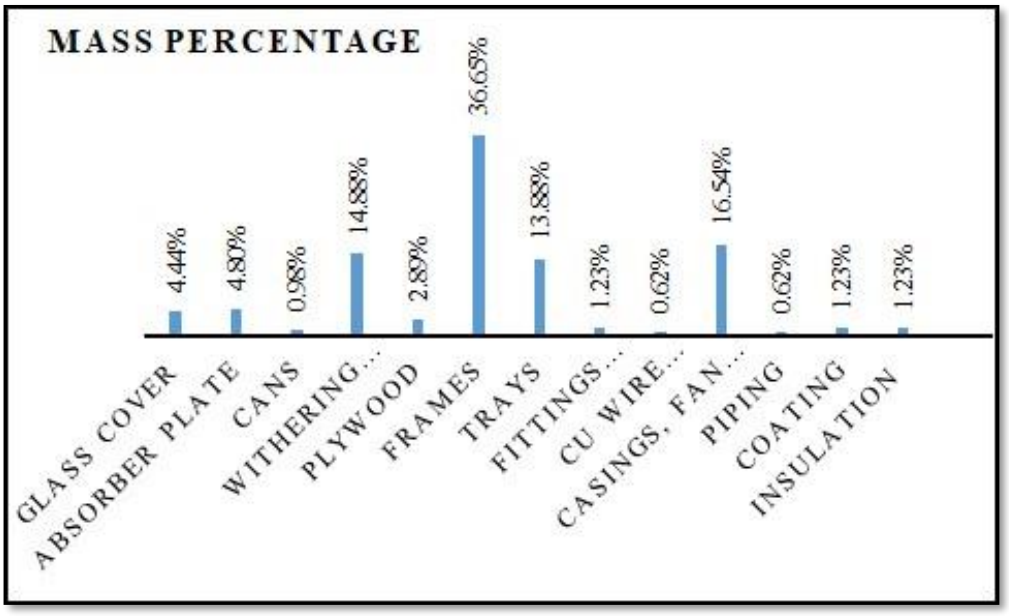

Fig. 6.16(a). Break-up of mass of the materials

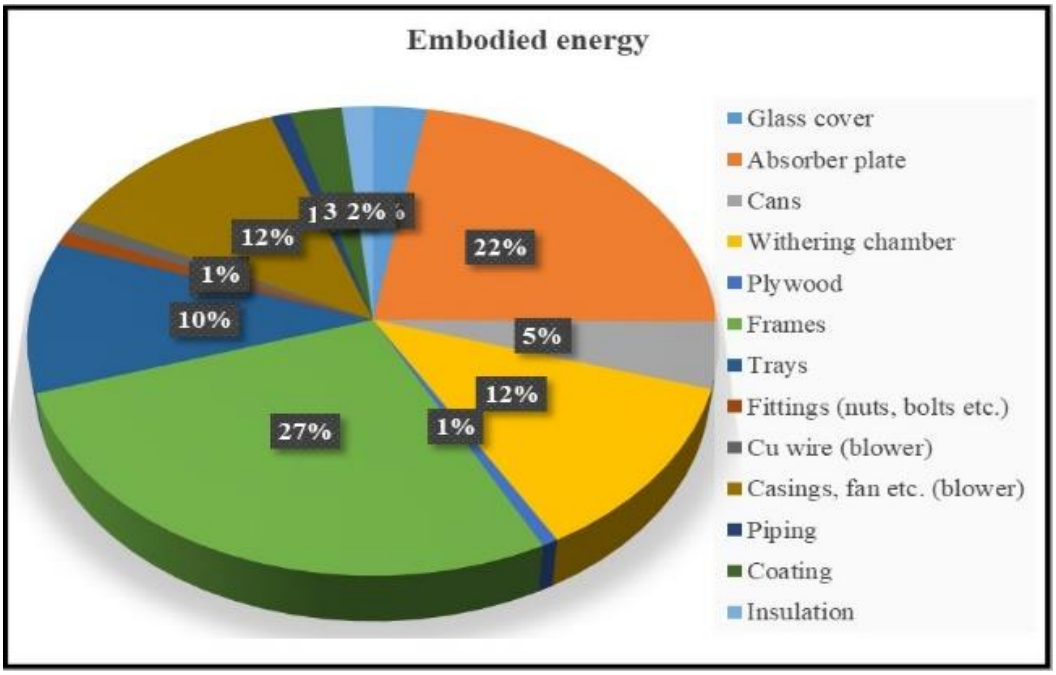

Fig. 6.16(b). Break-up of embodied energy

The moisture content in the tea leaves is required to reduce up to (55-60) % during the process of withering. If it decreases to 55%, the moisture evaporated is estimated as 4.5 kg. The latent heat of evaporation is considered as 2429.80 kJ/kg. The daily thermal output is estimated to be 3.04 kWh. The energy payback period is obtained as 1.26 years which is much lesser than the ultimate lifetime of the system, i.e., 20 years. This period is lower than that of an indirect solar dryer [191] and a passive greenhouse dryer [35]. The results obtained for CO_2 emission and mitigation for the lifespan of 5-20 years are tabulated in Table-6.6. The CO_2 emission and mitigation are comparable with those of [35,191]. The carbon credit earned for this lifespan is evaluated at the rate of (5-20) $/t of CO_2 mitigation and shown in Table-6.7. The earned carbon credits are again comparable with those evaluated for indirect solar dryers and greenhouse dryers [35,191].

Table-6.6. CO_2 emission and mitigation

Life (years)	**5**	**10**	**15**	**20**
CO_2 emission (kg/year)	392.06	196.03	130.69	98.01
CO_2 mitigation (t)	5.79	13.54	21.30	29.05

Table-6.7. Carbon credit earned

Life (years)	**5**	**10**	**15**	**20**
Carbon credit (at 5 $/t)	28.96	67.72	106.49	145.25
Carbon credit (at 20 $/t)	115.85	270.90	425.95	581.00

6.3 Conclusions

Green tea leaves were dried at low temperatures (withered) in a laboratory-scale tea withering trough equipped with an SAH with two different absorber plates- first with a corrugated plate and then with a plate incorporated with waste Al-can protrusions. The experiments were conducted using the mass flow rates of 0.03, 0.04 and 0.05 kg/s in both the cases. The energy, exergy and environmental assessments of the system were carried out. Following are the key observations concluded from the study-

- In the Type-1 SAH, the maximum temperatures at the outlet were 42.2 ℃, 49 ℃ and 46.6 ℃ for the mass flow rates of 0.03, 0.04 and 0.05 kg/s respectively. The corresponding maximum thermal efficiencies were 24.68%, 64.2% and 51.29% respectively.
- The exergy efficiencies in the Type-1 SAH varied within the ranges of (0.94-2.02) %, (1.61-3.82) %. and (1.88-3.8) % for the three flow rates.
- The exergetic efficiency of the Type-1 withering chamber varied from (25.98-81.09) %, (52.11-94.23) % and (44.65-92.2) % during the day at the respective flow rates considered.
- The best outlet temperatures obtained in the Type-2 SAH were 52.1 ℃, 58.7 ℃ and 53.2 ℃ for the mass flow rates of 0.03, 0.04 and 0.05 kg/s respectively. The maximum thermal efficiencies accordingly were 44.73%, 74.77% and 71.44%.
- For the three mass flow rates, the exergy efficiencies in the Type-2 SAH varied within the ranges of (1.87-3.16) %, (2.28-5.84) % and (2.81-5.49) %.
- The exergy efficiency variations in the Type-2 withering chamber went from (50.98-89.26) %, (69.06-95.63) % and (52.28-95.2) % for the three instances.
- The *THPP*s of both corrugated and Al-can SAH were above unity in average.
- The energy payback time for the Type-2 trough was estimated to be 1.26 years with earned carbon credit of 145.25 $ to 581 $ for a lifetime of 20 years.

It is clear from both the cases that the Type-2 SAH is more efficient for carrying out the tea-leaf withering process. Also, the preferable mass flow rate comes out to be 0.04

kg/s for the system. Moreover, the environmental analysis reflects that tea- withering based on solar thermal power is an environmentally sound process.

The last chapter of the thesis is a summary of the conclusions drawn from the entire study done on the prospect of intervening the tea-leaf withering process with solar thermal energy. Further, a future scope is highlighted to carry forward the study.